



Bachelor Thesis

# **Applying frequency scanning arrays for time-efficient analog beam probing in multi-user hybrid beamforming systems**

Eloi Gómez Martínez

Born on: Barcelona, Spain

in: 15/02/2000

Discipline: Elektrotechnik/ERASMUS

Matriculation number: 500215

to achieve the academic degree

**Bachelor**

First referee

Prof. Dr.-Ing. Dr. h.c. Gerhard Fettweis

Supervisor

Dipl.-Ing. Christoph Jans



**TECHNISCHE  
UNIVERSITÄT  
DRESDEN**

---

**Faculty of Electrical and Computer Engineering** Institute of Communication Technology  
Vodafone Chair Mobile Communications Systems

# Abstract

Next generation of mobile communications will have to cover the unceasingly growing demand of higher data rates and reliable services. In this situation it will be a must to migrate towards higher frequencies in the range of millimeter waves (mm-Waves), where there is plenty of available bandwidth, that would allow high data rates. However, for this new range of the spectrum the attenuation suffered is very strong. Therefore, the isotropic antennas used for lower frequencies are going to be replaced for highly directive ones in order to compensate for this effect. But at the same time the use of narrow beam will introduce a new problematic aspect that was previously inexistent, which is beam selection and beam alignment. In order to address this situation, efficient beamforming and beam alignment becomes critical.

The ultimate aim of this thesis is to test Frequency Scanning Arrays (FSA) for analog beam probing techniques in multi-user hybrid beamforming systems. In order to achieve it, several previous steps have been made.

This thesis is aiming to apply the technology of Frequency Scanning Arrays (FSA) in multi-user hybrid beamforming systems. First the analog beam probing using traditional Exhaustive Search (ES) is implemented, with not only hybrid but also analog and digital schemes. Also, several beam selection algorithms are defined and tested. Afterwards the effect of the channel estimation is considered and a timing delay for each user is implemented, in order to make the final comparison between ES and FSA as realistic as possible.

The results obtained show that in most cases analysed the FSA system outperforms the ES system. These encouraging results could be a good indicator that the use of FSA analog beam probing has many promising possibilities and has to be further investigated.

# Selbständigkeitserklärung Einzelarbeit

## *Statement of Authorship – Individual Thesis*

Ich versichere, dass ich die vorliegende Abschlussarbeit selbständig verfasst und keine anderen als die angegebenen Quellen und Hilfsmittel benutzt habe. Ich reiche sie erstmals als Prüfungsleistung ein. Mir ist bekannt, dass eine Täuschung mit der Note "nicht ausreichend" (5,0) geahndet wird.

*I hereby declare that I have written this final thesis independently and have listed all used sources and aids. I am submitting this thesis for the first time as a piece of assessed academic work. I understand that attempted deceit will result in the failing grade "not sufficient" (5.0).*

Name / Last Name:

Vorname / First Name:

Matrikelnummer / Student Number:

Datum / Date

Unterschrift / Signature

# Acknowledgements

I would like to thank my supervisor Christoph Jans, for his support and patience throughout the research. He has been very patient and constantly helped me by sharing his knowledge, ideas, and motivation.

I would like to express my gratitude towards Dr. Gerhard Fettweis for providing me with this amazing opportunity of a bachelor thesis at the Vodafone Chair of TU Dresden.

Last but not least, big thanks to my family and friends for supporting me all the time. This would not have been possible without you!

# Table of contents

<b>1</b>	<b>Introduction .....</b>	<b>10</b>
<b>2</b>	<b>Background review .....</b>	<b>11</b>
2.1	Millimeter Waves (mmWave).....	11
2.2	Beamforming.....	12
2.2.1	Analog Beamforming .....	12
2.2.2	Digital Beamforming.....	13
2.2.3	Hybrid Beamforming.....	13
2.3	Beam probing techniques .....	13
2.3.1	Exhaustive Search (ES) .....	14
2.3.2	Frequency Scanning Array (FSA).....	14
<b>3</b>	<b>System model .....</b>	<b>15</b>
3.1	Narrowband assumption.....	15
3.2	Input signal .....	16
3.3	System structure .....	16
3.4	Sum-rate calculation of the system.....	18
3.5	Attenuation parameter alpha.....	18
3.6	Timing delay.....	19
3.7	Channel matrix .....	19
3.7.1	Exhaustive Search (ES) .....	20
3.7.2	Frequency Scanning Array (FSA).....	21

<b>4</b>	<b>Results .....</b>	<b>23</b>
4.1	Analog beam selection algorithms .....	23
4.1.1	Greedy algorithm allowing collision (Algorithm 0).....	23
4.1.2	Greedy algorithm avoiding collision (Algorithm 1).....	24
4.1.3	Brute force algorithm (Algorithm 2) .....	24
4.1.4	Brute force algorithm enhanced (Algorithm 3).....	25
4.1.5	Algorithm comparison.....	26
4.2	Algorithm 0 vs Algorithm 1 .....	26
4.2.1	Full channel knowledge (Genie).....	27
4.2.2	Estimated channel knowledge .....	31
4.3	ES vs FSA.....	34
<b>5</b>	<b>Conclusions and future development: .....</b>	<b>42</b>

# List of Figures

Figure 2-1: Electromagnetic spectrum .....	11
Figure 2-2: Hybrid beamforming scheme. $N_D$ is he number of RF chains and $N_A$ is he number of antennas steered analogically per RF chain [5].....	13
Figure 3-1: Narrowband assumption .....	15
Figure 3-2: Schematic of the system structure, as in [8]. .....	17
Figure 4-1: Performance comparison between the several algorithms proposed.....	26
Figure 4-2: Genie, Alg.0, $L = 1$ .....	27
Figure 4-3: Genie, Alg.0, $L = 3$ .....	28
Figure 4-4: Genie, Alg.1, $L = 1$ .....	29
Figure 4-5: Genie, Alg.1, $L = 3$ .....	29
Figure 4-6: Estimate, Alg.0, $L = 1$ .....	31
Figure 4-7: Estimate, Alg.0, $L = 3$ .....	32
Figure 4-8: Estimate, Alg.1, $L = 1$ .....	33
Figure 4-9: Estimate, Alg.1, $L = 3$ .....	33
Figure 4-10: ES vs FSA; Alg. 0 & Analog; kshift = 0, $M=8$ .....	35
Figure 4-11: ES vs FSA; Alg. 0 & Analog; Random kshifts, $M=8$ .....	36
Figure 4-12: ES vs FSA; Alg. 0 & Analog; kshifts = 0, $M=64$ .....	36
Figure 4-13: ES vs FSA; Alg. 0 & Hybrid CB; kshift = 0, $M=8$ .....	37
Figure 4-14: ES vs FSA; Alg. 0 & Hybrid CB; Random kshifts, $M=8$ .....	37
Figure 4-15: ES vs FSA; Alg. 0 & Hybrid CB; kshift = 0, $M=64$ .....	37
Figure 4-16: ES vs FSA; Alg. 1 & Hybrid CB; kshift = 0, $M = 8$ .....	38
Figure 4-17: ES vs FSA; Alg. 1 & Hybrid CB; Random kshifts, $M=8$ .....	38
Figure 4-18: ES vs FSA; Alg. 1 & Hybrid CB; kshift = 0, $M= 64$ .....	38
Figure 4-19: ES vs FSA; Alg. 0 & Hybrid ZF; kshift = 0, $M=8$ .....	39
Figure 4-20: ES vs FSA; Alg. 0 & Hybrid ZF; Random kshifts, $M=8$ .....	39
Figure 4-21: ES vs FSA; Alg. 0 & Hybrid ZF; kshift = 0, $M=64$ .....	39
Figure 4-22: ES vs FSA; Alg. 1 & Hybrid ZF; kshift = 0, $M = 8$ .....	40
Figure 4-23: ES vs FSA; Alg. 1 & Hybrid ZF; Random kshifts, $M=8$ .....	40



Figure 4-24: ES vs FSA; Alg. 1 & Hybrid ZF; kshift = 0, M = 64 .....40

# 1 Introduction

The demand for better services in mobile communications is increasing at a very fast pace, powered by the generalisation use of smartphones, as well as all other type of gadgets that will require the use of this services. All these factors are already tightening the existing system. Up until now, only the bands below 6 GHz have been used to provide mobile communication services, but the above-mentioned increasing demand of services is making the transition to the higher frequency bands in the mm-Wave, which had never been previously used for wireless communications, a necessity. These new bands in the mm-Wave have large chunks of available spectrum, which would allow for higher bandwidths, therefore potentially enabling higher data-rate communications, as well as more reliable services. The main problem of these high frequency bands is the larger attenuation of the signals. This means that the path loss is much more important and the signals are easily blocked by obstacles and building, since its penetration capacity is severely decreased because of the shorter wavelengths, in the range of a few millimeters.

In order to overcome this problem, omnidirectional antennas used in sub-6GHz bands will have to be replaced by highly directional antennas able to create narrow beams in order to focus the transmitted signal power as concentrated as possible to the receiver [1]. In this situation beamforming becomes critical.

The use of directional antenna also introduces a new problem, which is the beam alignment between the transmitter and the receiver, and the beam selection process implied. This part becomes critical as well, because it is no use achieving very narrow beams if afterwards these beams are not pointed in the correct direction.

To address these challenges, in this thesis we propose several beamforming schemes along with several beam selection algorithms. In addition, we test these not only for the traditional beam probing system applying exhaustive search, but using frequency scanning arrays, a promising option that as stated in [2] is proved to considerably reduce the typically large timing overhead of beam alignment. This work will focus on analysing performance-wise both options in different types of environment in order to determine the optimal one in every situation.

## 2 Background review

In this section some theoretical concepts that are relevant to the topic of the Thesis are briefly introduced.

### 2.1 Millimeter Waves (mmWave)

Up until the fourth generation of mobile communications, the same range of frequencies has been used by mobile operators. The spectrum where all the wireless networks were included was below 6 GHz, in the so-called radio-frequency spectrum. Therefore, the bandwidth available is very limited, which in turn makes the services offered to be slower and of less quality.

A possible solution to cope with the high demand is to transmit signals on a new portion of the spectrum that has never been used for mobile communications in the past. The providers of services are exploring the possibility of broadcast transmission on millimeter-Waves (mm-Waves), that correspond to higher frequencies than the radio waves that have been traditionally used.

As seen in Figure 2-1, the mm-Waves are corresponded to the frequencies between 30 GHz and 300 GHz. The reason for its denomination of mm-Waves is that its wavelength ( $\lambda$ ) is on the order of a few millimeters, mostly between 1 mm and 10 mm. On the other hand, the wavelength of the radio waves used to serve smartphones nowadays is on the order of a few to tens of centimeters.

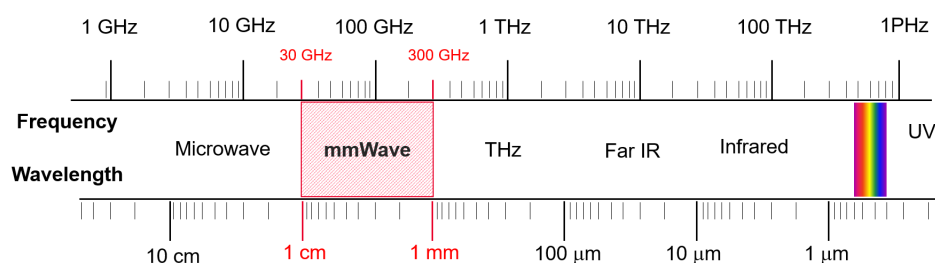


Figure 2-1: Electromagnetic spectrum

Despite the advantages mentioned above, mm-Wave have an important drawback. Due to the short wavelength, the signals transmitted on the mm-Wave range suffer a much stronger attenuation than the signals from the band below 6 GHz. Not only its path loss is considerably higher, but also its obstacle penetration loss. This means that they are easily blocked by all kind of buildings or obstacles.

However, the advances and improvements in the design of antennas and the short wavelengths of mm-Wave signals, relatively small devices can pack many (up to hundred) antennas in the form of antenna arrays. This factor allows for beamforming to be used in both transmitter and receiver to compensate the high channel attenuation suffered by the transmitted signal. Therefore, the wide spectrum available in the mm-Wave could be used to cover highly demanding services of the upcoming generations of mobile communications.

## **2.2 Beamforming**

To achieve higher data rate communication beamforming has been identified as an essential technology. It is utilized in communication within the mm-Wave range to ensure directional transmitted signals. This is achieved by altering the amplitude and phase of each one of the antennas of the antenna array. The combination of all the signals of the antenna elements results in a directed and narrow beam [3]. It is worth noticing the fact that the larger the number of antennas contained in the antenna array the narrower the beam achieved, therefore being able to direct the beam at a more exact location in space.

There are several beamforming schemes each used for different applications: analog, digital and hybrid beamforming.

### **2.2.1 Analog Beamforming**

When all elements of the antenna array are attached to a single radio frequency RF chain each, it is considered analog beamforming. High beamforming gains can be generated with large arrays in a simple and effective technique, even though it doesn't allow much flexibility.

Only a single RF chain is used, therefore this technique can only support one communication beam at a time, which implies a lower throughput [4].

### 2.2.2 Digital Beamforming

In full digital beamforming, each antenna element is connected to its corresponding RF chain. This allows for a high degree of freedom when combining the signals of each antenna element, as well as a magnificence performance. On the other hand, compared to the analog scheme the hardware complexity as well as the cost is considerably higher.

In this scheme, for each RF there are Fast Fourier Transform / Inverse Fast Fourier Transform (FFT/IFFT) blocks, digital to analog converters (A/D), and analog to digital converters [3].

### 2.2.3 Hybrid Beamforming

In figure 2-2 an example of hybrid beamforming is showed. As it can be observed, it is a combination of both analog and hybrid combinations. It has several RF chains, but much less than the number of antenna elements [5].

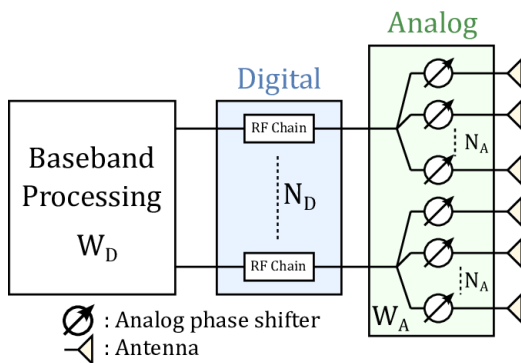


Figure 2-2: Hybrid beamforming scheme.  $N_D$  is he number of RF chains and  $N_A$  is he number of antennas steered analogically per RF chain [5].

## 2.3 Beam probing techniques

In this section, the two beam probing techniques used in this work are presented.

### 2.3.1 Exhaustive Search (ES)

Exhaustive search is the most commonly used beam probing technique that consists on sequentially testing a set of beamformers obtained from a codebook.

### 2.3.2 Frequency Scanning Array (FSA)

Frequency scanning arrays is a very widely used technology in the radar field, where it has been implemented using microstrip technology for several decades [6]. The frequency scanning array is a special case of the general phased array antennas. In FSA, the transmitter's frequency controls the beam steering without using any phase shifter. Therefore, the beam steering is a function only dependant on the frequency. By setting large timing delays of fixed multiples of the sampling time  $\tau_c = 1/f_B$ , it is possible to steer over the whole range  $\varphi \in [-\pi/2, \pi/2]$ .

It has only been in recent years that the interest in applying FSA to communications has significantly increased. In [2], FSA analog beam probing has been proved to drastically reduce the timing overhead needed to obtain the optimal beamformer. The key concept used is the mapping of spatial frequencies onto temporal frequencies, that allows to estimate the Angle of Departure (AoD) with a very small error with a single observation at each tested frequency.

### 3 System model

In this section the model used in the following simulations is detailed, including important parameters as well as assumptions that have been considered.

We use the following notation throughout this section:  $\mathbf{A}$  is a matrix,  $\mathbf{a}$  is a vector and  $a$  is a scalar.  $\mathbf{A}^T$  is the transpose of  $\mathbf{A}$ , whereas  $\mathbf{A}^*$ ,  $\mathbf{A}^{-1}$  are its Hermitian and inverse respectively.  $\mathbf{I}$  is the identity matrix.  $F(\mathbf{A})$  is the Fast Fourier Transform (FFT) of  $\mathbf{A}$  and  $F^{-1}(\mathbf{A})$  is the Inverse FFT of  $\mathbf{A}$ .  $F_s(\mathbf{A})$  is the FFT shift of  $\mathbf{A}$ , whereas  $F_s^{-1}(\mathbf{A})$  is the IFFT shift of  $\mathbf{A}$ .

#### 3.1 Narrowband assumption

One of the first things to consider is whether the narrowband assumption can be made in order to simplify the complexity of all further work. In order to prove that, we plot as in [7] the beam pattern using the Butler matrix for both no narrowband assumption (solid line) and narrowband assumption (dotted line).

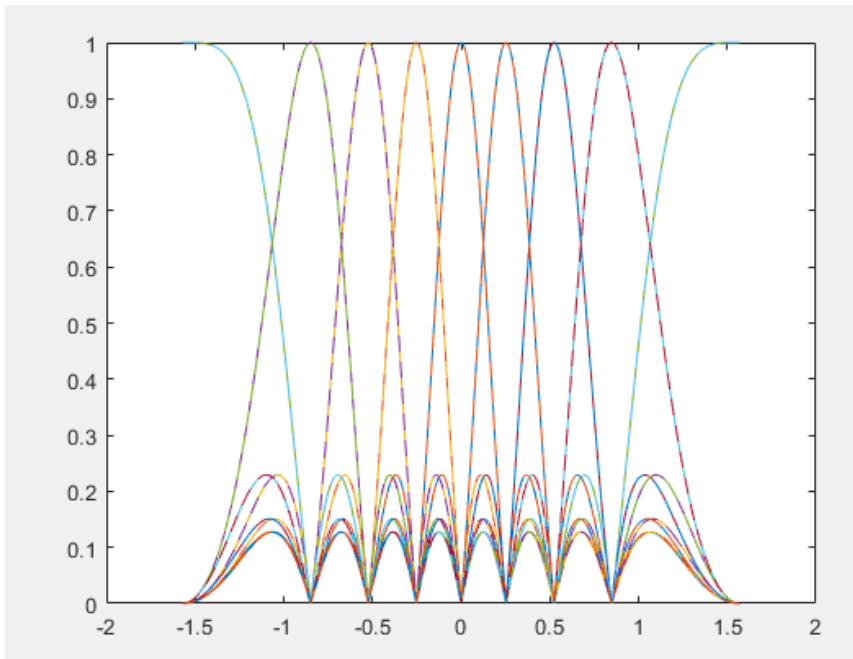


Figure 3-1: Narrowband assumption

From the graph can be observed that the solid and dotted line are completely superposed. This means that the narrowband assumption is feasible because of the large  $f_c/B$  ratio. The narrowband assumption is very useful and will be used in this work since it reduces the complexity of the conceptual and mathematical treatment of the situations analysed without much loss of accuracy.

## 3.2 Input signal

The input signal used in this work is the Zadoff-Chu sequence. The reason this signal has been used is because it has the property that if several versions of the sequence are cyclically shifted, they are all orthogonal to one another, as well because of the output of the signal has constant amplitude. This last feature is especially needed for the frequency scanning array (FSA), because since this system is frequency dependant, all frequencies used have to keep the same output power.

For example, if a short pseudorandom (PN) sequence was used, it could be the case that the power spectrum resultant didn't have a constant magnitude. This situation would introduce an undesired bias in the beam probing and beam selection processes.

The Zadoff-Chu is defined by the length of the sequence and its index. The defined length is  $K$  (number of baseband sampling points), and index  $K-1$ . This value selected fulfil the requirement that the length and index have to be coprime (relatively prime).

## 3.3 System structure

The system structure used in this work is based on the one defined in [8]. In this work we will also consider a multi-user mmWave downlink (DL) system model consisting on a single BS that uses hybrid (analog + digital) precoding and an antenna array in order to give service to  $U$  MSs. In this work however, for the sake of simplicity we will consider that each MS has only one single RF (analog) chain instead of an RF Combiner with several RF chains (as stated in the figure below).



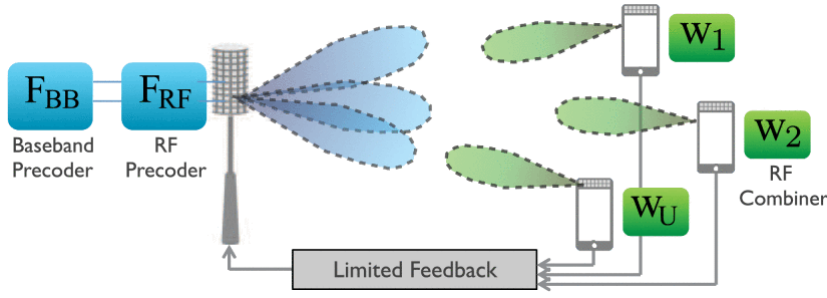


Figure 3-2: Schematic of the system structure, as in [8].

$F_{BB} = [f_1^{BB}, f_2^{BB}, \dots, f_U^{BB}]$  is a  $U \times U$  matrix, which parametrizes the digital part of the transmitter TX, as represented in Figure 2-2.

$F_{RF} = [f_1^{RF}, f_2^{RF}, \dots, f_U^{RF}]$  is a  $M \times U$  matrix, which parametrizes the analog part of the transmitter TX, as represented in Figure 2-2.

$H$  is the channel matrix, of dimensions  $U \times M$ .

$\mathbf{h}_u$  is a vector of length  $M$ .  $\mathbf{h}_u$  is the  $u$  column of the channel matrix  $H$

Where  $M$  is the number of antennas in the antenna array in the base station (BS)

In the analog scheme, as it has been mentioned in 2.2.1, there is only one RF chain. Therefore, the Baseband Precoder is transparent ( $F_{BB\_analog} = I$ ) and the resulting analog beamformer consists only on the RF Precoder:

$$W_{analog} = F_{RF} F_{BB\_analog} = F_{RF} \quad (1)$$

In the fully digital and hybrid schemes we will consider two beamforming techniques, Conjugate Beamforming (CB) and Zero Forcing (ZF):

- CB technique, where the  $F_{BB}$  is calculated taking the Hermitian of the effective channel matrix:

$$F_{BB\_hybrid} = H_{eff}^* \quad (2)$$

- ZF technique, where the  $F_{BB}$  is calculated as follows:

$$F_{BB\_hybrid} = H_{eff}^* (H_{eff} H_{eff}^*)^{-1} \quad (3)$$

In our downlink scenario (DL), ZF technique allows the base station (BS) to send data to the selected users while nulling out the direction of the rest of the users.

In both cases, the effective channel matrix is

$$\mathbf{H}_{eff} = \mathbf{H}\mathbf{W}_{analog} \quad (4)$$

Finally, the resulting Hybrid beamformer is the following:

$$\mathbf{W}_{hybrid} = \mathbf{W}_{analog}\mathbf{F}_{BB\_hybrid} \quad (5)$$

### 3.4 Sum-rate calculation of the system

A metric has to be defined in order to evaluate the overall performance of the system. Using the system model in [8], the following rate for each user  $u$  is defined:

$$R_u = \log_2 \left( 1 + \frac{\frac{P}{U} |\mathbf{h}_u \mathbf{F}_{RF} \mathbf{f}_u^{BB}|^2}{\frac{P}{U} \sum_{n \neq u} |\mathbf{h}_u \mathbf{F}_{RF} \mathbf{f}_n^{BB}|^2 + \sigma^2} \right) \quad (6)$$

Where  $P$  is the total power of the system and  $U$  the total number of users.

Then the sum-rate of the system is  $R_{sum} = \sum_{u=1}^U R_u$ .

In order to improve this metric, we will seek to design the analog and digital precoders at the base station (BS) as efficiently as possible.

In this work we will consider that the total power  $P$  is unitary ( $P = 1$ ), as well as uniformly distributed among all users.

### 3.5 Attenuation parameter alpha

An attenuation parameter has to be defined in order to quantize the attenuation the signal suffers when travelling from the BS to the MS through the channel. Following the notation used in [9], we define the following expression for each element of the attenuation parameter  $\alpha$ , which has dimensions of  $1 \times L$ , where  $L$  is the number of paths.

$$\alpha_l = \sqrt{\gamma_l} \left( \sqrt{\frac{\eta_l}{\eta_l + 1}} + \sqrt{\frac{1}{1 + \eta_l}} \right) \left( \frac{a_l + jb_l}{\sqrt{2}} \right) \quad (7)$$

where

- $\mathbf{a}, \mathbf{b}$  are  $1 \times L$  vectors, where each element follows a normal Gaussian distribution
- $\boldsymbol{\gamma}$  is a  $1 \times L$  vector which represents the overall multipath component strength
- $\boldsymbol{\eta}$  is a  $1 \times L$  vector which represents the strength ratio between LOS and NLOS

In all the simulation included in this work we have considered  $\boldsymbol{\gamma} = \begin{bmatrix} 1 \\ 0.1 \\ 0.1 \end{bmatrix}$  (strong direct component) and  $\boldsymbol{\eta} = \begin{bmatrix} 100 \\ 10 \\ 0 \end{bmatrix}$ .

### 3.6 Timing delay

A random circular shift to the input signal has been applied to all  $L$  paths of each user.

By implementing this timing delay, we make our system more realistic because the users are most probably not at the same distance to the BS. Therefore, due to the longer or shorter transmission time caused by the variable proximity of the UEs to the BS, the first sample of the signal received by each UE will be different. In our implementation we consider that each signal path received by each user starts with a random sample. This is equivalent to considering all UEs are randomly distributed around the BS and, in the effect of multi-path, both LoS and NLoS components travel a random distance before arriving to the user.

In this case, the notation used for the circular shifted input signal is  $\mathbf{x}_s$  instead of  $\mathbf{x}$ .

### 3.7 Channel matrix

This implementation of the channel matrix showed in this section is based on [8].

$$\mathbf{h}_u = \alpha e^{-2j\pi f_c \tau_d} e^{-2j\pi f_c \left(m - \frac{M-1}{2}\right) \frac{d}{c} \sin(\phi)} \quad (8)$$

Where,  $\alpha$  is the attenuation parameter as defined in 3.6,  $f_c$  is the carrier frequency of the signal,  $\tau_d$  is the timing delay of the antenna array associated to each path of the signal,  $d$  is the distance between elements of the antenna array (set to  $\lambda/2$ ),  $c$  is speed of light and  $\phi$  is the Angle of Departure of the signal (AoD) for each path.  $M$  is the number of antennas in the array and  $\mathbf{m} = [0 \ 1 \ 2 \ \dots \ M - 1]^T$ .

### 3.7.1 Exhaustive Search (ES)

$$\mathbf{h}_{\text{eff\_ES},i} = \mathbf{h}_u^T \sqrt{\frac{1}{M}} e^{-j2\pi(f_c)(\frac{1}{f_c})\mathbf{m}(\frac{i}{M})} \quad (9)$$

Where:

$i = 0, 1, 2, \dots, M - 1$  is the number of the selected beam

$$\mathbf{r}_{ES} = \mathbf{H}_{\text{eff\_ES}} \mathbf{x} \quad (10)$$

$$\mathbf{y}_{ES} = \mathbf{r}_{ES} + \mathbf{z} \quad (11)$$

Where  $\mathbf{z}$  is a vector of length  $L$ , and each element is complex random Gaussian noise value of variance  $N_0/2$ .

**Without circular shift as specified in 3.6**

We estimate the effective channel  $\mathbf{h}_{eff\_ES}$  by minimizing its mean square error (MSE)  $E|\mathbf{h}_{eff\_ES} - \widehat{\mathbf{h}}_{eff\_ES}|^2$  based on the over-sampled and noisy observations  $\mathbf{y}_{ES}$ . Therefore, we use the classical linear minimum mean square error (LMMSE) estimator [10].

$$\widehat{\mathbf{h}}_{eff\_ES} = (\mathbf{x}\mathbf{x}^*)^{-1} \mathbf{x}^* \mathbf{y}_{ES} \quad (12)$$

**With circular shift as specified in 3.6**

$$\widehat{\mathbf{h}}_{eff\_ES} = \sqrt{\sum \left| \frac{\mathbf{x}_s * \mathbf{y}_{ES}}{K} \right|^2} \quad (13)$$

In this case with circular shift, the previous LMMSE estimator cannot be used. Therefore, we obtain the estimation of the effective channel using the cross-correlation between the shifted input signal  $\mathbf{x}_s$  and the noisy observations  $\mathbf{y}_{ES}$ .

### 3.7.2 Frequency Scanning Array (FSA)

The implementation of the Frequency Scanning Array showed in this section is based on [11].

Step 1

$$W_l(f) = \sum_{m=0}^{M-1} e^{jm2\pi(\tau_{tt,d,l} - \frac{d}{c} \sin \phi_l)(f+f_c)} \quad (14)$$

Where  $\tau_{tt,d,l} = m/B$ , which allows us to steer over the complete range of  $\varphi \in [-\pi/2, \pi/2]$  as explained in 2.3.2

$$\mathbf{W}_l = [W_l(-B/2) \quad \dots \quad W_l(B/2)] \quad (15)$$

Step 2

$$\mathbf{r}_{FSA} = \frac{\alpha_l}{M} \mathbf{W}_l \text{diag}(e^{-2j\pi(f_c+f)\tau_d}) \tilde{\mathbf{S}} \quad (16)$$

$$\tilde{\mathbf{S}} = \text{diag}(\mathbf{S}_{FSA}) [\mathbf{A}, \dots, \mathbf{A}]. \quad (17)$$

The matrix  $\mathbf{A}$  is repeated  $K * M$  times, where  $K$  is the number of baseband sampling points and  $M$  the number of antennas contained in the antenna array.

$$\mathbf{S}_{FSA} = \frac{1}{M} \mathbf{F}_s \mathbf{F} \mathbf{F}_s^{-1} (\mathbf{x}^T) \quad (18)$$

$$\mathbf{A} = \frac{1}{M} e^{-2j\pi \mathbf{F}_s^{-1} \left( \frac{\mathbf{k}^T \mathbf{k}}{M} \right)} \quad (19)$$

Where  $\mathbf{k} = [0 \ 1 \ 2 \ \dots \ M - 1]$ ,  $\mathbf{x}$  is the input signal as defined in 3.2,  $\mathbf{F}$  is the Fast Fourier Transform (FFT),  $\mathbf{F}_s$  is the FFT shift and  $\mathbf{F}_s^{-1}$  is the Inverse FFT shift.

Then the complex random noise  $\mathbf{z}$  is added

$$\mathbf{y}_{FSA} = \mathbf{r}_{FSA} + \mathbf{z} \quad (20)$$

Now the efficient channel matrix is calculated, both considering full channel knowledge (using the signal transmitted) and the estimated channel knowledge (using the signal transmitted with the added gaussian complex noise)

$$\mathbf{h}_{EFF\_FSA} = \mathbf{r}_{FSA} \tilde{\mathbf{S}}' (\tilde{\mathbf{S}} \tilde{\mathbf{S}}')^{-1} \quad (21)$$

$$\widehat{\mathbf{h}}_{EFF\_FSA} = \mathbf{y}_{FSA} \tilde{\mathbf{S}}' (\tilde{\mathbf{S}} \tilde{\mathbf{S}}')^{-1} \quad (22)$$

## 4 Results

In this section the results of all the simulations carried out during the development of this work are presented.

### 4.1 Analog beam selection algorithms

First of all, several analog beam selection algorithms have to be tested and compared in order to conclude which one is more adequate.

For the algorithms described below, all the following simulation parameters had the same value in order to be able to make a fair comparison between them:

- A uniform linear array (ULA) of  $M = 32$  antennas with carrier frequency  $f_c = 60 \text{ GHz}$ , bandwidth  $B = 1 \text{ GHz}$  and distance between antenna elements  $d = c/(2f_c)$
- One channel path,  $L = 1$ , meaning line-of-sight (LoS)
- Uniformly distributed AoD:  $\phi \sim U[-\pi/2, \pi/2]$
- The transmitted signal is of duration  $T = K/B$ , with  $K = 64$  sampling points and sampling duration of  $T_s = 1/B$ .
- The number of users in the system is  $UE = 3$ .

#### 4.1.1 Greedy algorithm allowing collision (Algorithm 0)

In this algorithm, the system is designed to maximize the signal power of each user, not considering the interference among them. This means that each user selects the beam that gives the higher signal power, neglecting the possible collision between users that choose the same beam.

By not avoiding beam collision between users, the interference is considerably high, mostly caused by the cases where the interference is caused by another user using the same beam. On top of that, this situation could lead to practical problems on a hardware level because several beams would have to be pointed in the same direction.

#### 4.1.2 Greedy algorithm avoiding collision (Algorithm 1)

In this algorithm, the system is designed to maximize the signal power of each user, but avoiding the beam collision among users.

For each iteration we make a sweep among all the users and establish the beam preferences of each of them. Then, if the beam used by the reference user collides with another user using the same beam with a higher amplitude, then the reference user switches its beam to the next on specified in the beam preference array. Otherwise, the reference user keeps its selected beam. Therefore, we obtain a collision free user-beam combination for each iteration. This way we significantly reduce the interference, because the worst interference scenario of 2 or more users using the same beam is avoided. Consequently, the spectral efficiency of the system is increased.

#### 4.1.3 Brute force algorithm (Algorithm 2)

In this case, we test all of the possible beams for the number of users (UE). Then, for each case the performance criteria is calculated following the expression defined in 3.4

An important disadvantage of this method is that the execution time is extremely high, because it has to test all different beam configurations. For the values we have of  $M=8$  antennas in the array and  $\#UE = 3$ , we have to test all the combinations of 3 elements in a group of 8 elements, including all the possible permutations for each combination. Therefore, in total we have  $\binom{8}{3} = 56$  combinations multiplied by 6 permutations possible in each group of 3 elements. That makes a total of 336 configurations that have to be tested for each single iteration. This process has to be repeated for all the iterations within every noise value  $N_0$ . And for the values used of 100 iterations and 9 noise values, the total amount of different configurations tested adds up to  $336 \times 100 \times 9 = 302.400$ . Finally for each one the sum-Rate is calculated, and the optimal configuration with higher sum-Rate value is selected.

The execution takes 506,6 seconds, which is 8 minutes and 26,6 seconds.

A consideration has to be made if the improvement achieved is worth the huge increase in time required.



#### 4.1.4 Brute force algorithm enhanced (Algorithm 3)

This Algorithm is based on the Algorithm 2 (Brute force), but it is implemented differently so that the execution time is drastically reduced while keeping a high spectral efficiency.

In this Algorithm, we don't test each and every possible combination of beams selected by the users for every iteration. The previous brute force Algorithm is not efficient, because most of all the beam combinations tested have very low efficiency, therefore we spend a lot of time testing beam combinations that we know from beforehand will never be selected.

So in this case, for each iteration we create an array of beam preferences of each user as explained in 4.1.2. A matrix of the beam preferences of all the users is created. Then we test all the possible combinations of beams, which are all the possible combinations of the beams in each of the beam-preference array of each user. All these combinations are stored in a matrix, where each file is a combination of beams to be tested.

An example with 2 users could be the following:

UE1 has beam 3 as first preference and beam 4 as second preference.

UE2 has beam 5 as first preference and beam 6 as second preference.

Matrix of "Beam preferences":  $\begin{bmatrix} 3 & 4 \\ 5 & 6 \end{bmatrix}$

Matrix of "All possible combinations of beams":  $\begin{bmatrix} 3 & 5 \\ 3 & 6 \\ 4 & 5 \\ 4 & 6 \end{bmatrix}$

We can already observe that this Algorithm3 will be much more efficient than Algorithm 2, because the combinations of beams has already been preselected among the optimal beams for each user. This way we avoid spending computational time calculating the sumRate for cases that will give low spectral efficiency.

### 4.1.5 Algorithm comparison

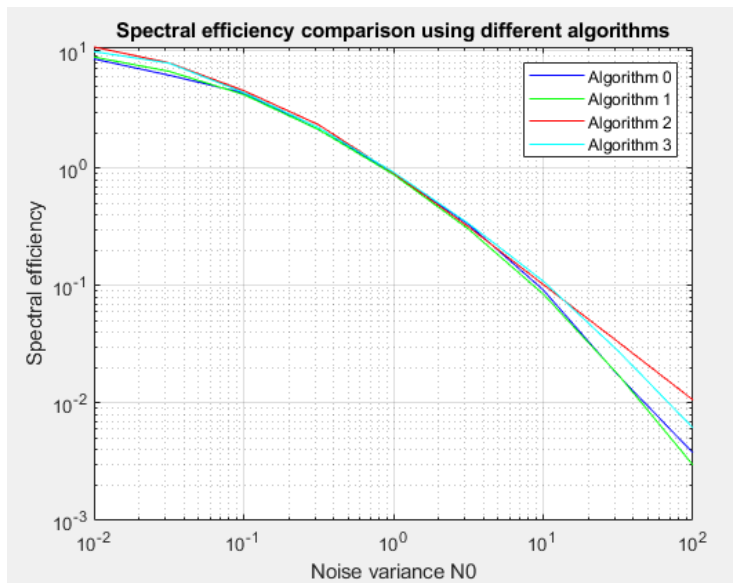


Figure 4-1: Performance comparison between the several algorithms proposed

We observe that the algorithm that achieves the higher sum-rate is Algorithm 2, followed by Algorithm 3, and then Algorithm 1 and Algorithm 0 very close with each other. But as it is mentioned in 4.1.3, Algorithm 2 takes an extremely long amount of time to execute because of the huge number of cases that have to be tested in comparison to the other Algorithms. Therefore, the preferred algorithm is Algorithm 3, because it achieves a nearly as good spectral efficiency as Algorithm 2, but using a considerably shorter amount of time.

## 4.2 Algorithm 0 vs Algorithm 1

In this section we evaluate the performance of the several beamforming schemes for as well as two of the algorithms presented in 4.1, Algorithm 0 (allowing beam collision) and Algorithm 1 (avoiding beam collision). The performance parameter is the Sum-rate defined in 3.4.

The following simulation parameters will be fixed in order to guarantee a fair comparison:

- The number of used samples of the pilot sequence length will be  $K = 256$
- The number of users is  $UE = 6$
- The number antennas in the antenna array is  $M = 32$
- Multi-path:

- Single-path ( $L = 1$ )
- Multi-path ( $L = 3$ )

#### 4.2.1 Full channel knowledge (Genie)

- **Case 1: Sum-rate with full knowledge of the channel**
  - Pure analog beamforming scheme
    - Greedy algorithm allowing collision (blue solid line)
  - Pure digital beamforming scheme as upper bound
    - Zero-Forcing (orange solid line)
    - Conjugate Beamforming (purple dotted line)
  - Hybrid beamforming setup
    - Greedy algorithm allowing collision + Zero-Forcing (yellow dotted line)
    - Greedy algorithm allowing collision + Conjugate Beamforming (green dotted line)

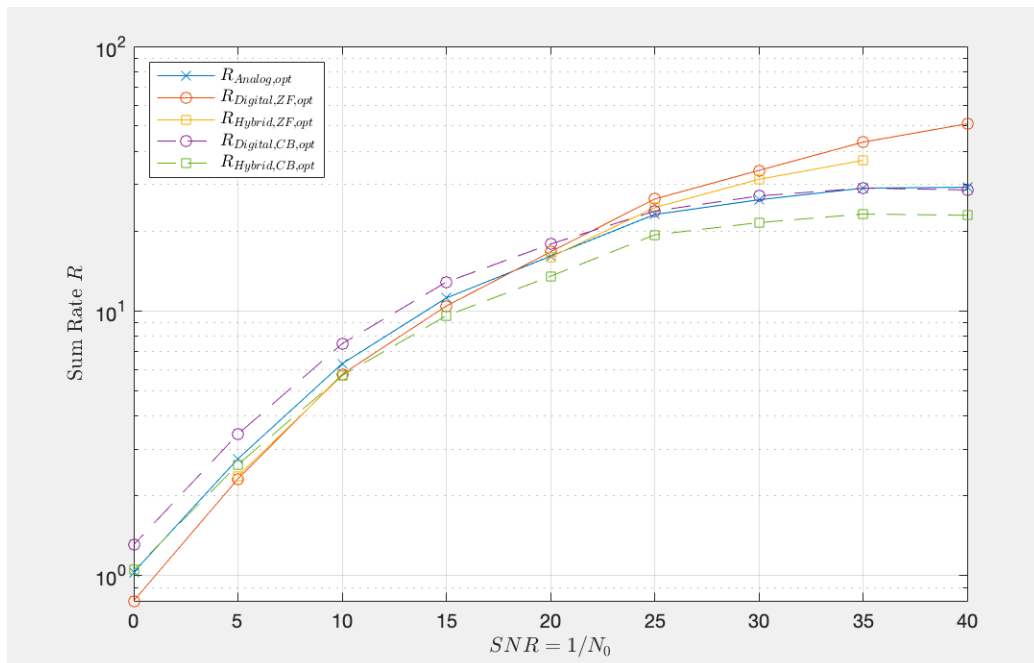


Figure 4-2: Genie, Alg.0,  $L = 1$

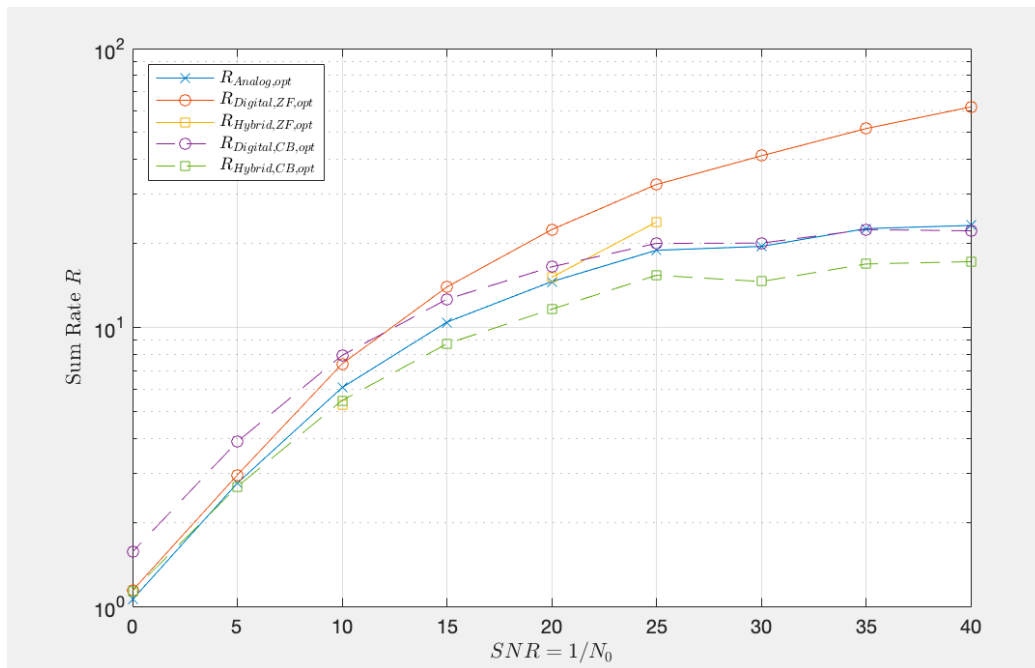


Figure 4-3: Genie, Alg.0, L = 3

- **Case 2: Sum-rate with full knowledge of the channel**
  - Pure analog beamforming scheme
    - Greedy algorithm preventing collision (blue solid line)
  - Pure digital beamforming scheme as upper bound
    - Zero-Forcing (orange solid line)
    - Conjugate Beamforming (purple dotted line)
  - Hybrid beamforming setup
    - Greedy algorithm preventing collision + Zero-Forcing (yellow dotted line)
    - Greedy algorithm preventing collision + Conjugate Beamforming (green dotted line)

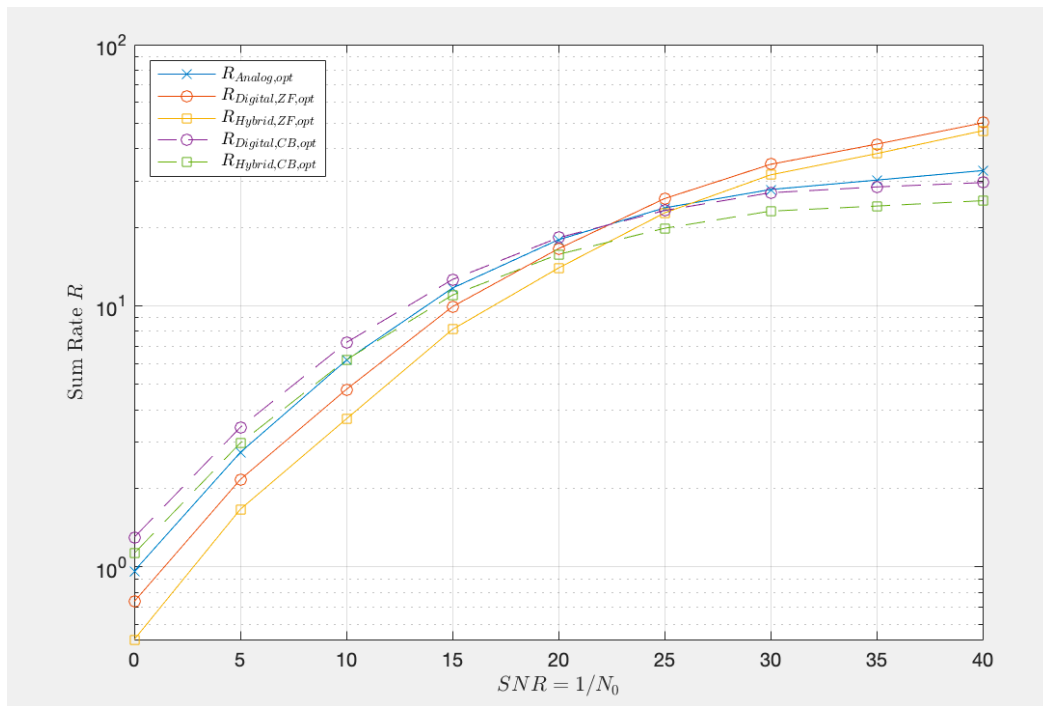


Figure 4-4: Genie, Alg.1, L = 1

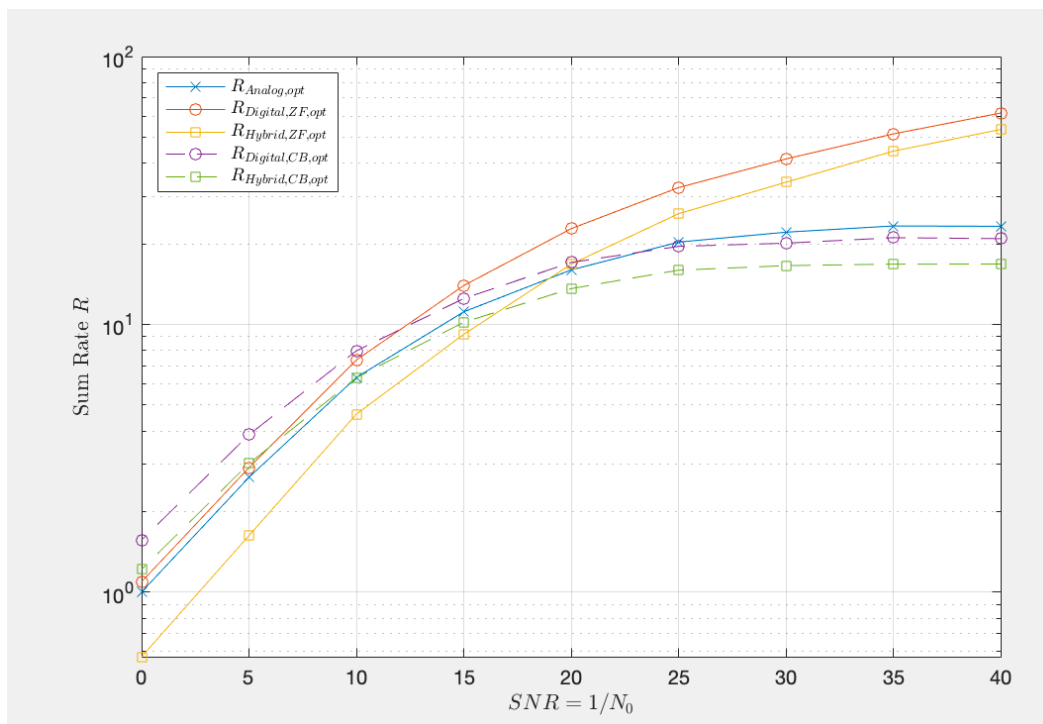


Figure 4-5: Genie, Alg.1, L = 3

**Case 1 (Fig. 4-2 & Fig. 4-3) vs Case 2 (Fig. 4-4 & Fig. 4-5):**

The first observation to be made is that, for the same value of  $L$ , the performance of the pure digital scheme remains the same because it is not affected by the different analog beam selection algorithm.

The performance of most of the schemes tested are very lightly affected by the algorithm used. The only observation to be made is that the Hybrid ZF scheme is severely affected by the beam collision even though its trend line follows the Digital ZF only a few dB below. For many executions the result of the inverse matrix needed for the Hybrid ZF is close to singular and therefore its values tend to infinity and are treated as NaN. That is the reason why some yellow points on both graphs of case 1 are missing.

On the other hand, in case 2, since the beam collision is avoided, there is no longer the execution issue explained above and all the values are obtained correctly.

 **$L = 1$  (Fig. 4-2 & Fig. 4-4) vs  $L = 3$  (Fig. 4-3 & Fig. 4-5):**

We observe a clear pattern for both  $L = 1$  and  $L = 3$ : for low SNR values until 20 dB, Analog and CB schemes perform better than ZF, but after 20 dB ZF schemes improve considerably over Analog and CB.

The difference observed is that for  $L = 3$  the improvement rate of the ZF scheme is higher than for  $L = 1$ , but the opposite for Analog and CB schemes. The explanation for this to happen is that when multi-path is introduced ( $L > 1$ ) and therefore channel information is increased; ZF can use it in order to distribute the power among users more efficiently thanks to its more degrees of freedom. On the other hand, Analog and CB don't have any way to make use of this multi-path, therefore its performance is reduced because the non-direct paths only contribute to interference.

## 4.2.2 Estimated channel knowledge

- **Case 1: Sum-rate with estimate of the channel**
  - Pure analog beamforming scheme
    - Greedy algorithm allowing collision (blue solid line)
  - Pure digital beamforming scheme as upper bound
    - Zero-Forcing (orange solid line)
    - Conjugate Beamforming (purple dotted line)
  - Hybrid beamforming setup
    - Greedy algorithm allowing collision + Zero-Forcing (yellow dotted line)
    - Greedy algorithm allowing collision + Conjugate Beamforming (green dotted line)

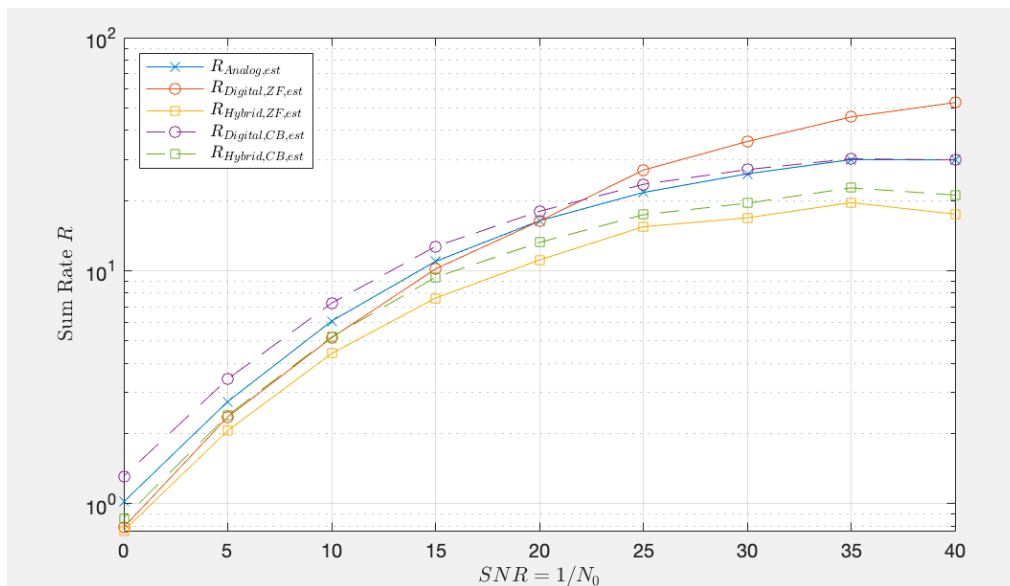


Figure 4-6: Estimate, Alg.0,  $L = 1$

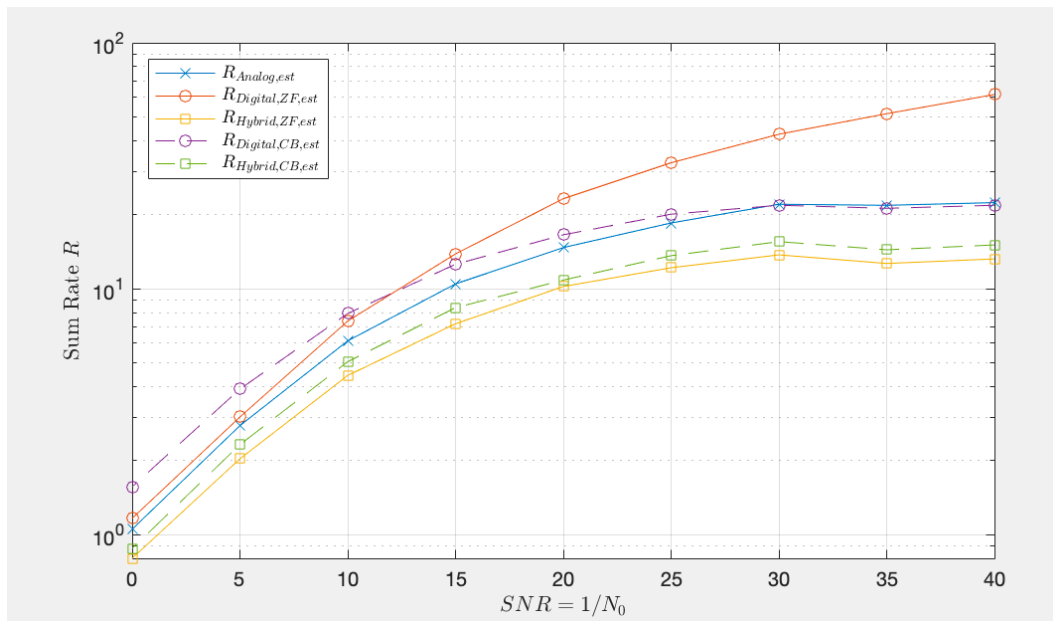


Figure 4-7: Estimate, Alg.0, L = 3

- **Case 2: Sum-rate with estimate of the channel**
  - Pure analog beamforming scheme
    - Greedy algorithm preventing collision (blue solid line)
  - Pure digital beamforming scheme as upper bound
    - Zero-Forcing (orange solid line)
    - Conjugate Beamforming (purple dotted line)
  - Hybrid beamforming setup
    - Greedy algorithm preventing collision + Zero-Forcing (yellow dotted line)
    - Greedy algorithm preventing collision + Conjugate Beamforming (green dotted line)



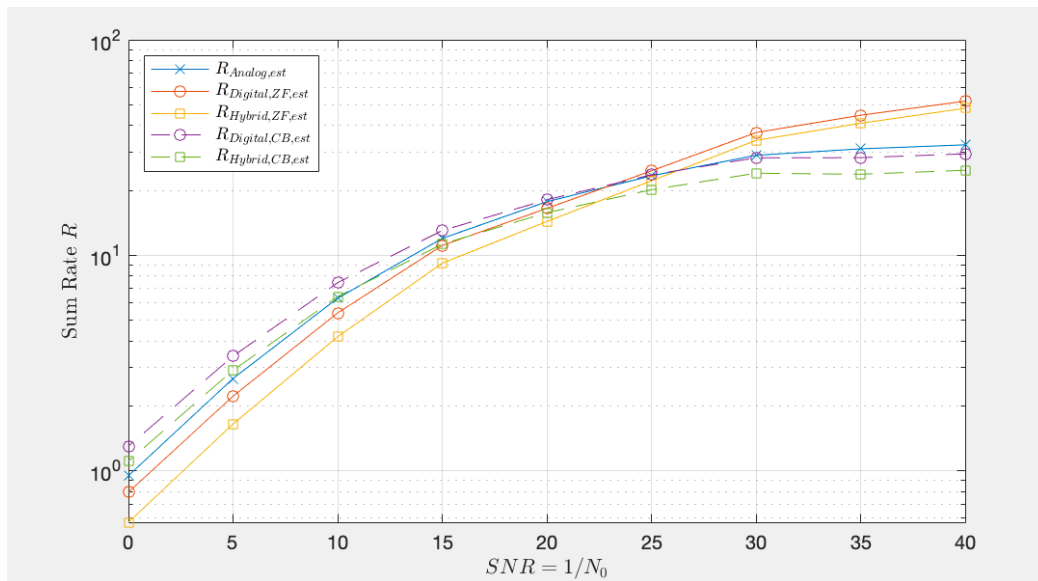


Figure 4-8: Estimate, Alg.1, L = 1

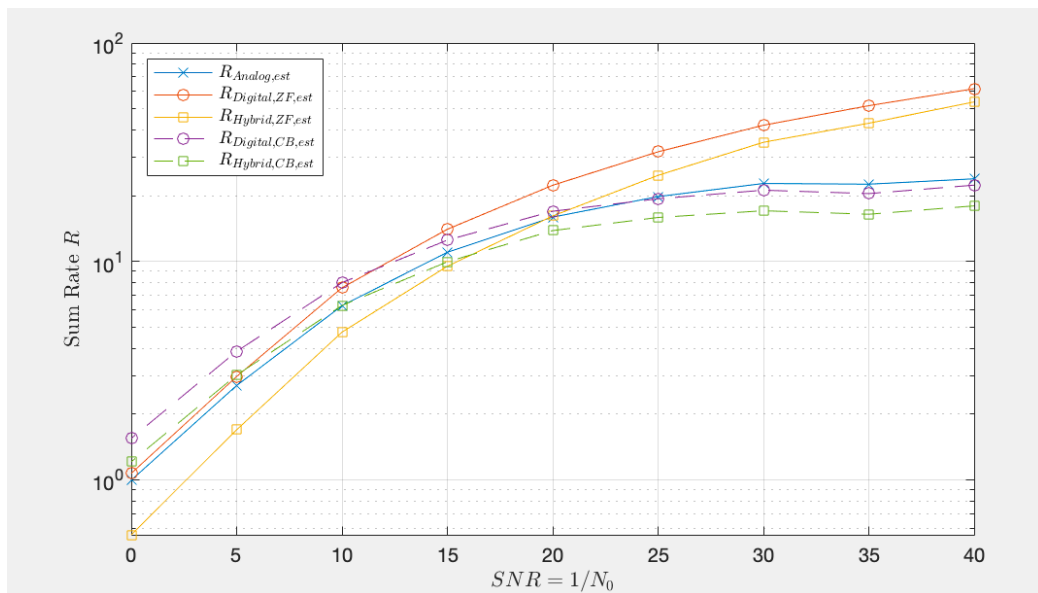


Figure 4-9: Estimate, Alg.1, L = 3

As in the previous section, for the same value of L, the performance of the pure digital scheme remains the same because it is not affected by the different analog beam selection algorithm.

An interesting difference to be observed is that there is a clear effect of the algorithm used for the Hybrid ZF scheme. The performance of the Hybrid ZF scheme using Algorithm 0 (Fig. 4-6 & Fig. 4-7) is the lowest of all the schemes analysed, but when changing to Algorithm 1 (Fig. 4-8 & Fig. 4-9) its performance improves drastically becoming the second best only under the Digital scheme. From these observations it can be concluded that when there is collision between beams, Hybrid ZF performance is very limited. On the other hand, when the beam collision is avoided, it can make use of its more degree of freedom to distribute the power among users efficiently and therefore outperforming both Analog and Hybrid CB schemes, that are barely affected by the change of algorithm and perform very similarly for both cases.

We also observe that in the multipath case  $L = 3$  (Fig. 4-7 & Fig. 4-9) Hybrid ZF schemes significantly improve compared to the single path case  $L = 1$  (Fig. 4-6 & Fig. 4-8), but Analog and Hybrid CB schemes perform slightly worse.

Therefore, it can be concluded that in terms of performance the ZF scheme avoiding beam collision is the preferred one. On the other hand, the main drawback of the ZF is that it is considerably more computationally costly than the CB because of the need to calculate the inverse of matrices compared to just having to calculate the Hermitian of these same matrices, as explained in 3.3.

### 4.3 ES vs FSA

Up until this moment, all the work has been focused on testing the different algorithms and beamforming schemes using Exhaustive Search (ES). But it is also of great interest testing the performance of the Frequency Scanning Array (FSA) and compare it to the ES, in order to get a sense of how both methods perform in the same conditions.

The comparison will only consider the Analog and Hybrid schemes because, as mentioned in 4.2, the Digital scheme is not affected by the beam selection algorithm.

In order to make the simulations in the most realistic way possible, we have used the estimated channel knowledge as defined in 3.6, and added a timing delay in the received signals implemented as a random circular shift as defined in 3.7.

For the results showed below, the following simulation parameters were used:

- A uniform linear array (ULA) of  $M = \{8, 64\}$  antennas with carrier frequency  $f_c = 60 \text{ GHz}$ , bandwidth  $B = 1 \text{ GHz}$  and distance between antenna elements  $d = c/(2f_c)$
- One channel path,  $L = 1$ , meaning line-of-sight (LoS)
- Uniformly distributed AoD:  $\phi \sim U[-\pi/2, \pi/2]$
- The transmitted signal is of duration  $T = K/B$ , with  $K = 10$  sampling points and sampling duration of  $T_s = 1/B$ .
- The number of users in the system is  $UE = 3$ .
- Timing delay introduced with a random circular shift  $kshift$  as explained in 3.6

In the results showed hereunder the color legend used in each simulation is the following:

- Optimal: blue line
- Exhaustive Search (ES): orange line
- Frequency Scanning Array (FSA): yellow line

#### Algorithm 0 (allowing collision) Analog scheme

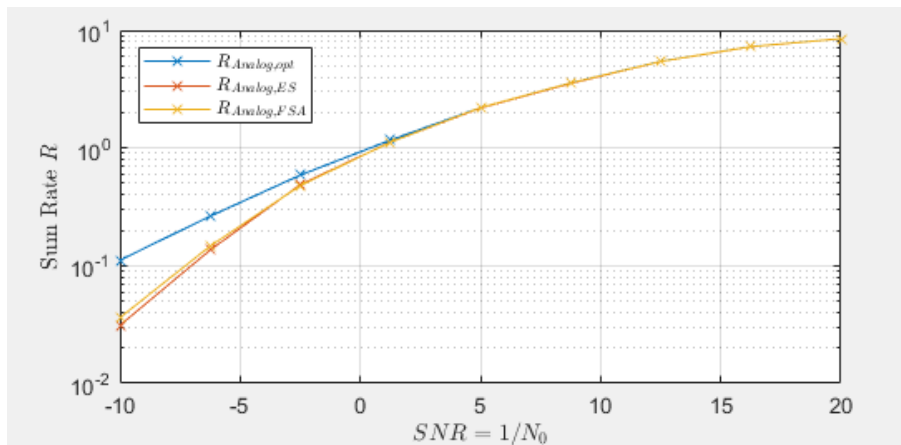


Figure 4-10: ES vs FSA; Alg. 0 & Analog; kshift = 0, M=8

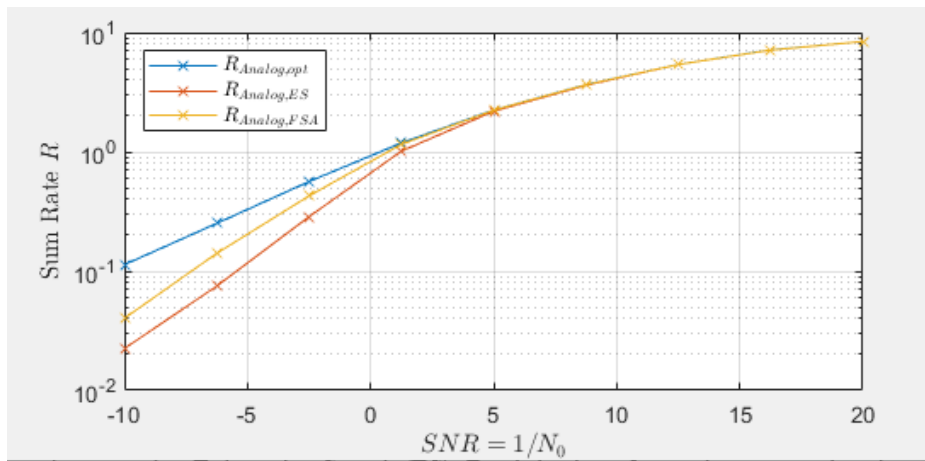


Figure 4-11: ES vs FSA; Alg. 0 & Analog; Random kshifts, M=8

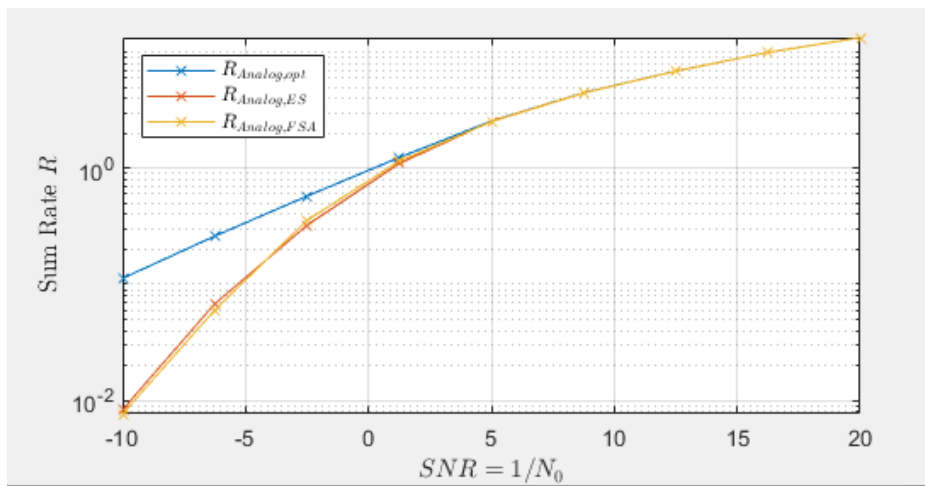


Figure 4-12: ES vs FSA; Alg. 0 & Analog; kshifts = 0, M=64

### Algorithm 0 (allowing collision) Hybrid CB

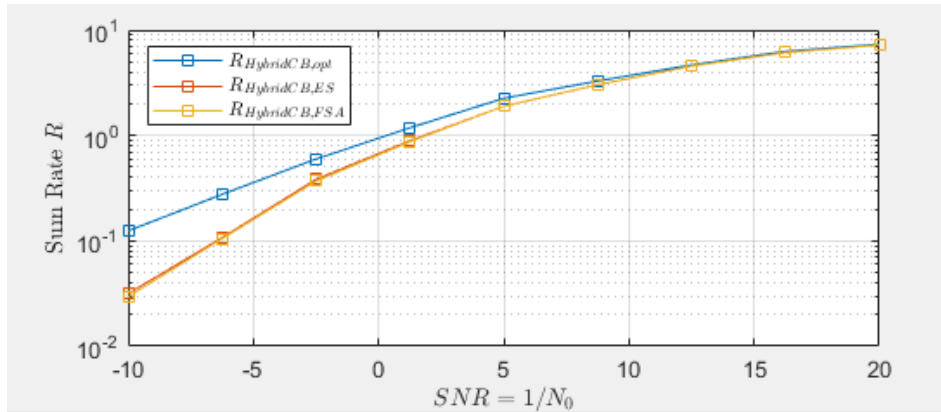


Figure 4-13: ES vs FSA; Alg. 0 & Hybrid CB; kshift = 0, M=8

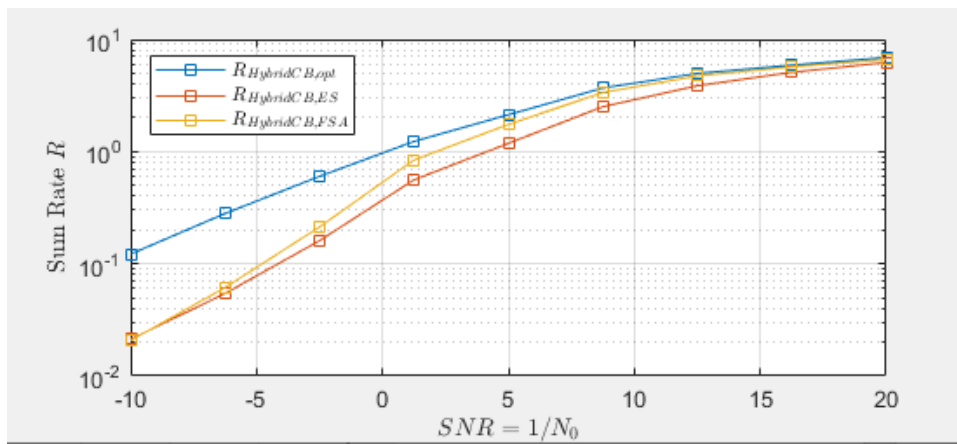


Figure 4-14: ES vs FSA; Alg. 0 & Hybrid CB; Random kshifts, M=8

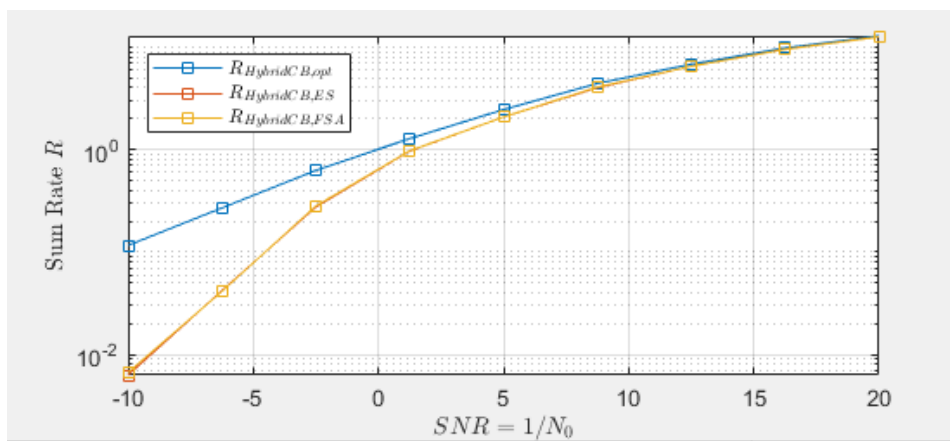


Figure 4-15: ES vs FSA; Alg. 0 & Hybrid CB; kshift = 0, M=64

### Algorithm 1 (preventing collision) Hybrid CB

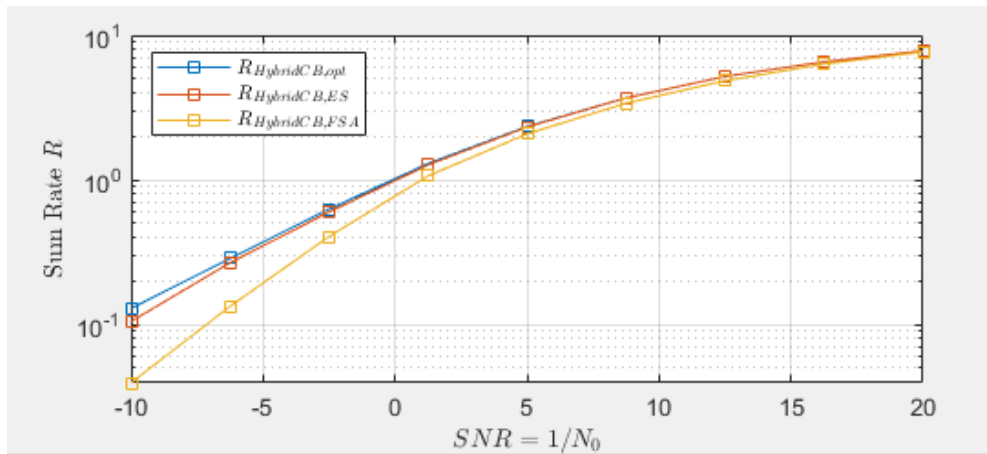


Figure 4-16: ES vs FSA; Alg. 1 & Hybrid CB; kshift = 0, M = 8

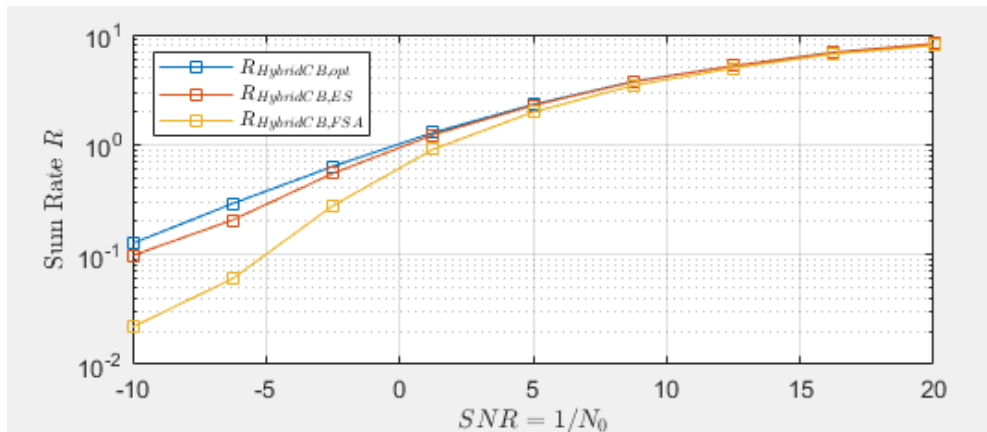


Figure 4-17: ES vs FSA; Alg. 1 & Hybrid CB; Random kshifts, M=8

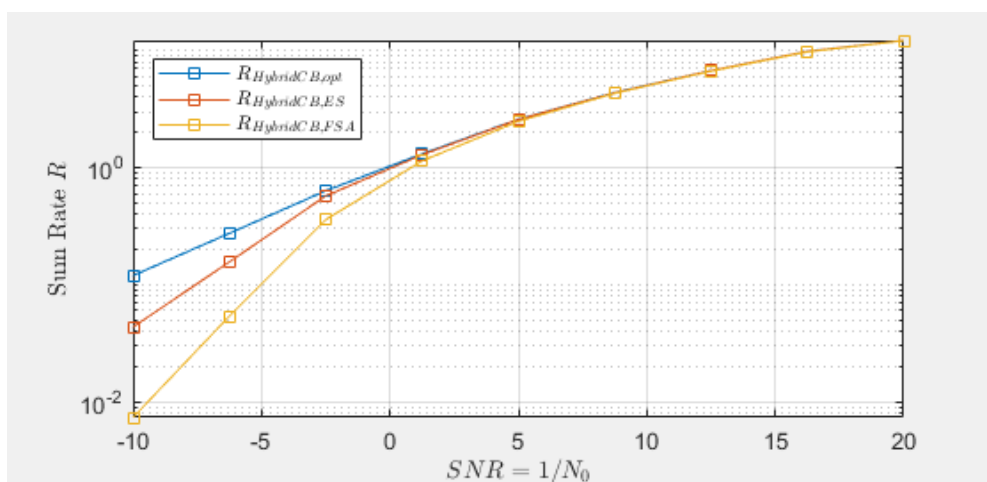


Figure 4-18: ES vs FSA; Alg. 1 & Hybrid CB; kshift = 0, M= 64

### Algorithm 0 (allowing collision) Hybrid ZF

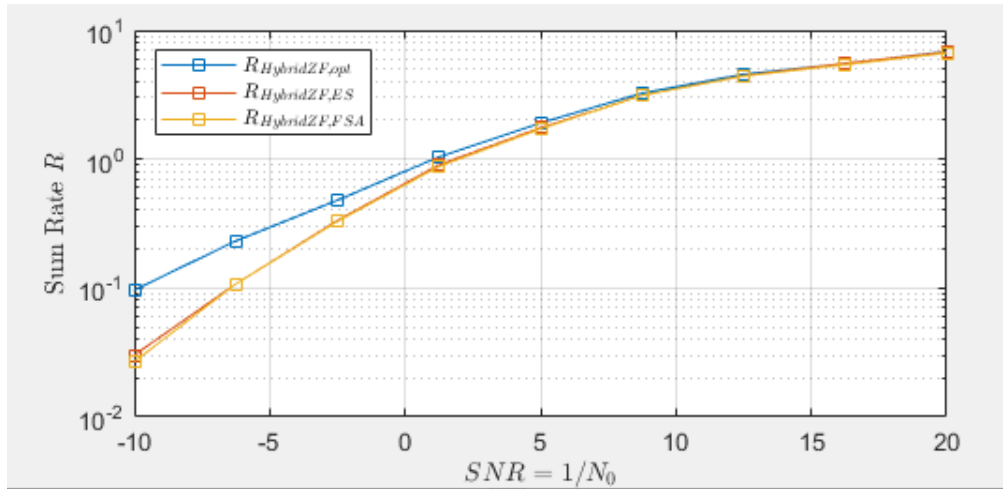


Figure 4-19: ES vs FSA; Alg. 0 & Hybrid ZF; kshift = 0, M=8

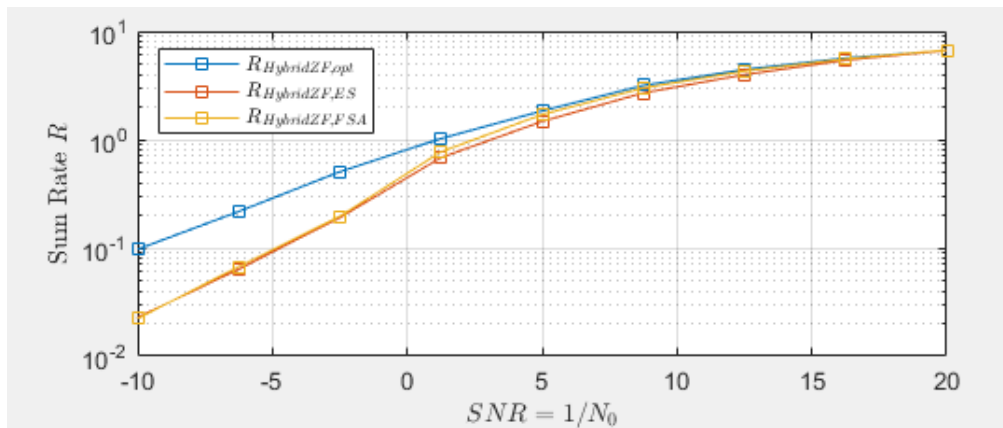


Figure 4-20: ES vs FSA; Alg. 0 & Hybrid ZF; Random kshifts, M=8

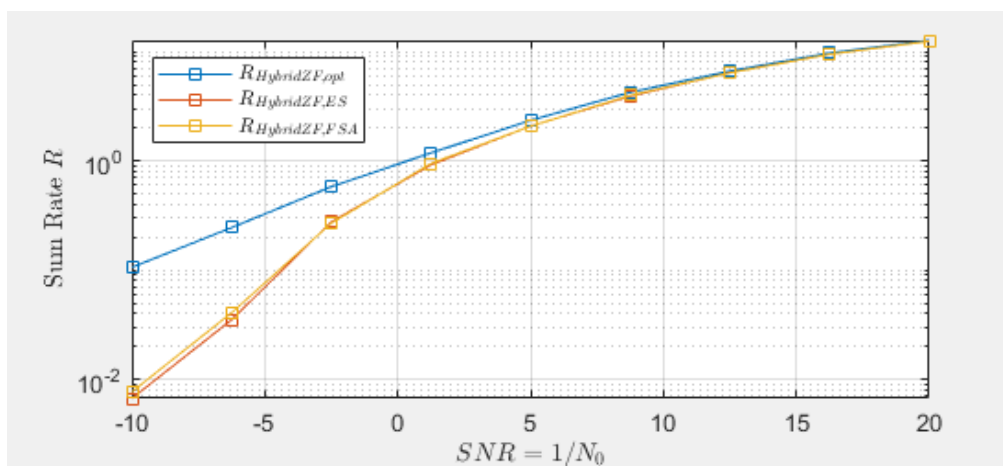


Figure 4-21: ES vs FSA; Alg. 0 & Hybrid ZF; kshift = 0, M=64

### Algorithm 1 (preventing collision) Hybrid ZF

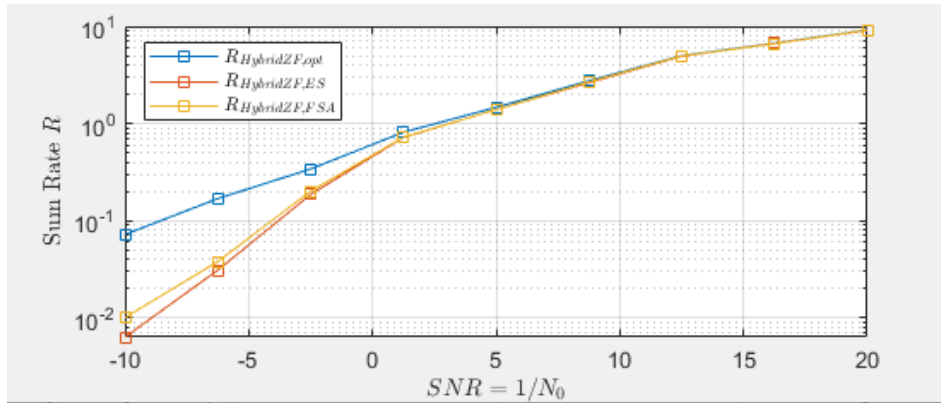


Figure 4-22: ES vs FSA; Alg. 1 & Hybrid ZF; kshift = 0, M = 8

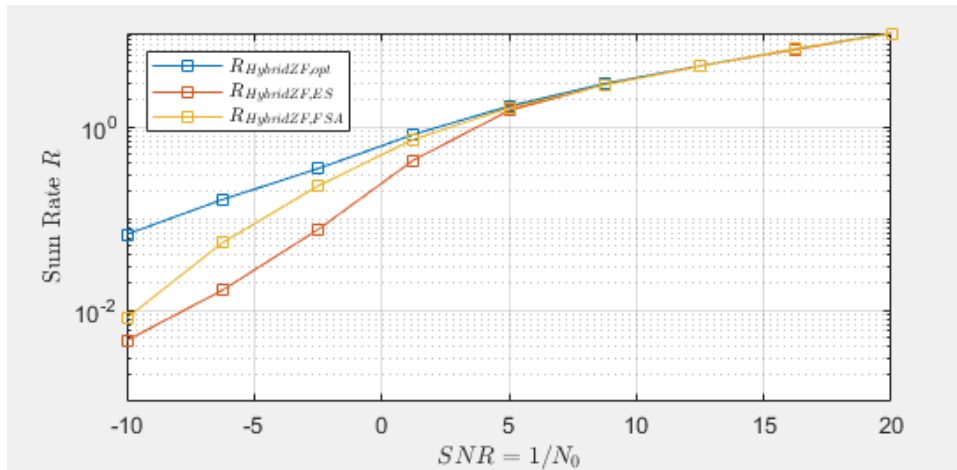


Figure 4-23: ES vs FSA; Alg. 1 & Hybrid ZF; Random kshifts, M=8

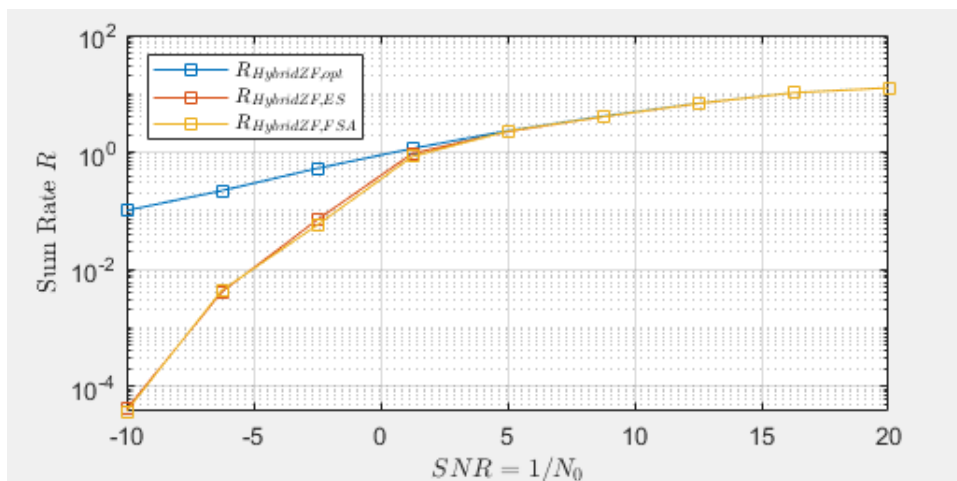


Figure 4-24: ES vs FSA; Alg. 1 & Hybrid ZF; kshift = 0, M = 64



## Summary and conclusions

- **Analog with collision (Fig. 4-10, 4-11, 4-12):**

ES and FSA have a similar performance without any timing offset.

When adding the random timing offset, the FSA consistently outperforms ES for low SNR (values  $< 0$  dB).

The case for Analog without collision has not been showed above because its results are very similar to the case with collision.

- **Hybrid CB with collision (Fig. 4-13, 4-14, 4-15):**

ES and FSA have a similar performance without any timing offset.

When adding the random timing offset, the FSA slightly overperforms for values of SNR  $> 0$  dB (very little)

- **Hybrid CB without collision (Fig. 4-16, 4-17, 4-18):**

ES overperforms FSA, especially for low SNR (values  $< 0$  dB) both with and without timing offset.

- **Hybrid ZF with collision (Fig. 4-19, 4-20, 4-21):**

ES and FSA have a similar performance for all SNR values both with and without timing offset.

- **Hybrid ZF without collision (Fig. 4-22, 4-23, 4-24):**

ES and FSA have a similar performance for all SNR values without any timing offset.

FSA overperforms ES for low SNR values ( $< 0$  dB).

For all the cases tested in this section, the single-path ( $L = 1$ ) and multi-path ( $L = 3$ ) simulations in each scheme offer very similar results. Therefore, only the single-path results have been presented.

We can observe that by making the ratio  $UE/M$  extremely low ( $UE = 3$ ,  $M = 64$ ), both in the CB and ZF cases, for low SNR values the spectral efficiency is considerably lower than for the cases of higher  $UE/M$  ratio ( $UE = 3$ ,  $M = 8$ ), but in both cases the trend lines achieve almost the same spectral efficiency than the optimal situation at SNR = 1 dB.

## 5 Conclusions and future development:

The importance of mobile communications is growing at a high pace in our society, therefore requiring its necessary development towards more efficient systems and higher data rates. The increasing number of users that have to be served everywhere has made the use of mmWave a necessity. Communications on the mmWave range offers a wide chunk of unused spectrum, but it comes at the cost of considerably higher path-loss and penetration loss than in lower frequencies. Due to this effect, highly directive beams have to be achieved in order to compensate the higher losses mentioned. Therefore, efficient beamforming is of crucial importance in order to achieve fast and precise beam alignment, as well as high transmission rates.

In this work the focus has been on exploring the possibilities of frequency scanning arrays (FSA) in multi-user hybrid beamforming systems to achieve time-efficient analog beam probing.

In the first part of this thesis several beam selection algorithms have been designed and tested. The overall result is that the most efficient algorithm was Algorithm 2, since it tested all possible beam combinations for the required number of users UE. This optimal performance had though an important inconvenience. The beam selection process was extremely long because even for a small number of users and array dimensions, the number of possible combinations to be tested mounted up to hundreds of thousands. Therefore, the preferred algorithm was Algorithm 3, since it obtained almost as good results as Algorithm 2 but in a much shorter amount of time. This was thanks to a pre-selection of the best beams for each user so that only the combinations with high probability of success were tested.

Afterwards the performance of several beamforming schemes was tested for Algorithm 0 and Algorithm 1 both using the ideal case of full channel knowledge and the realistic case of channel estimation. For the channel estimation, an important improvement was observed when using Algorithm 1 compared to the Algorithm 0 for the Hybrid ZF. This proves that in a realistic situation without full channel knowledge avoiding beams collision makes a huge difference in the performance of this scheme. All the other schemes analysed didn't present any noticeable changes in this aspect.

Up until this moment, only the traditional Exhaustive Search (ES) system had been used for analog beam probing. In the last part of this thesis an analog beam probing system based on Frequency Scanning Arrays (FSA) was implemented. An extensive test was made in order to compare the performance of ES and FSA for all the schemes and algorithms previously presented. To make this comparison as realistic as possible, not only the channel estimations were used, but also a random timing delay for each sequence received by the users to account for its different locations around the Base Station (BS), and therefore different travel time of the signal. The results obtained showed that without timing delay ES and FSA systems performed very similarly. When adding the random timing delay, in general the FSA system performed better, with the exception of the Hybrid CB using Algorithm 1, where the ES system performed better than the FSA in all cases.

As a general conclusion, from the investigations presented we have learned that the most promising scheme is the Hybrid Zero Forcing (ZF) for the beam selection algorithm that avoids collision. It provides near-optimal performance close to the fully digital scheme, while keeping a lesser complex structure than the latter, which facilitates an affordable and less energy-consuming hardware implementation. Regarding the beam probing technique, the FSA has been proven to provide a better performance on most of the schemes analysed, therefore making this technique preferable to the traditional ES.

Algorithms 2 and 3 were not implemented due to lack of time, but it would be of great interest to further test them in order to investigate how these algorithms would perform for the several beamforming schemes proposed, as well for the ES and FSA systems.

In this work the ideal case of no sidelobes on our beams has been considered in order to simplify the complexity of the implementations made. In order to get a more realistic environment these sidelobes should be considered because they introduce interference that could not be negligible.

In this thesis FSA and ES were only compared from a spectral efficiency/sum-rate point of view. In order to have a wider consideration of these beam probing systems could be very interesting to try to quantify the beam alignment time improvement of the FSA in respect to ES, which would be an important aspect to consider in order to have a broader and more fair comparison of both techniques.

# References:

- [1] T. S. Rappaport, R. W. Heath, R. C. Daniels, and J. Murdock, *Millimeter Wave Wireless Communications*. Englewood Cliffs (Prentice-Hall), 2014.
- [2] C. Jans, X. Song, W. Rave, and G. Fettweis, 'Fast Beam Alignment through Simultaneous Beam Steering and Power Spectrum Estimation Using a Frequency Scanning Array', in *WSA 2020; 24th International ITG Workshop on Smart Antennas*, 2020, pp. 1–6.
- [3] W. Roh *et al.*, 'Millimeter-wave beamforming as an enabling technology for 5G cellular communications: theoretical feasibility and prototype results', *IEEE Communications Magazine*, vol. 52, no. 2, pp. 106–113, 2014, doi: 10.1109/MCOM.2014.6736750.
- [4] J. Palacios, D. De Donno, and J. Widmer, 'Tracking mm-Wave channel dynamics: Fast beam training strategies under mobility', in *IEEE INFOCOM 2017 - IEEE Conference on Computer Communications*, 2017, pp. 1–9. doi: 10.1109/INFOCOM.2017.8056991.
- [5] A. Rozé, M. Crussière, M. Héland, and C. Langlais, 'Comparison between a hybrid digital and analog beamforming system and a fully digital Massive MIMO system with adaptive beamsteering receivers in millimeter-Wave transmissions', in *2016 International Symposium on Wireless Communication Systems (ISWCS)*, 2016, pp. 86–91. doi: 10.1109/ISWCS.2016.7600880.
- [6] M. Danielsen and R. Jorgensen, 'Frequency scanning microstrip antennas', *IEEE Transactions on Antennas and Propagation*, vol. 27, no. 2, pp. 146–150, 1979, doi: 10.1109/TAP.1979.1142049.
- [7] M. K. Marandi, W. Rave, and G. Fettweis, 'Beam Selection Based on Sequential Competition', *IEEE Signal Processing Letters*, vol. 26, no. 3, pp. 455–459, 2019, doi: 10.1109/LSP.2019.2895287.
- [8] A. Alkhateeb, G. Leus, and R. W. Heath, 'Limited Feedback Hybrid Precoding for Multi-User Millimeter Wave Systems', *IEEE Transactions on Wireless Communications*, vol. 14, no. 11, pp. 6481–6494, 2015, doi: 10.1109/TWC.2015.2455980.
- [9] X. Song, S. Haghghatshoar, and G. Caire, 'Efficient Beam Alignment for Millimeter Wave Single-Carrier Systems With Hybrid MIMO Transceivers', *IEEE Transactions on Wireless Communications*, vol. 18, no. 3, pp. 1518–1533, 2019, doi: 10.1109/TWC.2019.2892043.
- [10] S. Kay, *Fundamentals of statistical signal processing, vol. II: Detection Theory*. Prentice Hall, 1998.

- [11]M. Khalili Marandi, C. Jans, W. Rave, and G. Fettweis, 'Evaluation of Detection Accuracy and Efficiency of Considered Beam Alignment Strategies for mmWave Massive MIMO Systems', in *2021 55th Asilomar Conference on Signals, Systems, and Computers*, 2021, pp. 664–671. doi: 10.1109/IEEECONF53345.2021.9723262.